

## BENDING OF SUBMERGED WOODY RIPARIAN VEGETATION AS A FUNCTION OF HYDRAULIC FLOW CONDITIONS

MARK C. STONE<sup>a\*</sup>, LI CHEN<sup>b</sup>, S. KYLE MCKAY<sup>c</sup>, JOHN GOREHAM<sup>d</sup>, KUMUD ACHARYA<sup>b</sup>,  
CRAIG FISCHENICH<sup>c</sup> and ASAKO B. STONE<sup>f</sup>

<sup>a</sup> *Department of Civil Engineering, University of New Mexico, Albuquerque, New Mexico, USA*

<sup>b</sup> *Division of Hydrologic Sciences, Desert Research Institute, Las Vegas, Nevada, USA*

<sup>c</sup> *US Army Corps of Engineers, Engineer Research and Development Center, Athens, Georgia, USA*

<sup>d</sup> *Matson & Associates, State College, Pennsylvania, USA*

<sup>e</sup> *US Army Corps of Engineers, Engineer Research and Development Center, Vicksburg, Mississippi, USA*

<sup>f</sup> *Central New Mexico Community College, Albuquerque, New Mexico, USA*

### ABSTRACT

Woody riparian vegetation provides numerous ecological benefits such as stabilizing streambanks, storing and cycling nutrients, shading streams and providing habitat for wildlife. However, vegetation also increases hydraulic roughness and reduces the effective flow area, resulting in an increased water surface elevation for a given streamflow. Balancing the desire to preserve woody vegetation in stream corridors with the need to manage flood risks requires accurate techniques for predicting the influence of vegetation on stream hydraulics. However, this is a challenging problem because woody vegetation responds to the flow field itself by bending and streamlining in response to hydraulic forces. The goal of this study was to predict the bending behaviour of woody riparian vegetation as a function of hydraulic flow conditions. Field tests were performed to elucidate tree biomechanical properties for select riparian taxa of the southwestern USA. Biomechanical results served as input parameters for a numerical algorithm designed to predict tree bending for water velocities likely to be encountered during flood events. Bending simulations revealed appreciable variability in bent tree heights. Variability was likely a manifestation of the extensive variance in plant characteristics and properties inherent in biological specimens. However, no trees were expected to bend to a height lower than approximately 42% of their original height, even in water moving at  $2.5 \text{ m}\cdot\text{s}^{-1}$ . The results of this work provide an important first step in an effort to predict a dynamic hydraulic roughness for vegetated channels and floodplains under flood conditions. Copyright © 2011 John Wiley & Sons, Ltd.

KEY WORDS: riparian vegetation; hydraulic roughness; flood hydraulics; stream restoration; arid hydrology

Received 10 March 2011; Revised 12 July 2011; Accepted 26 July 2011

### INTRODUCTION

Today, it is widely recognized that past river engineering and economic water resources development practices, although often meeting specific project objectives, tended to work against nature rather than with it, and the consequence in many cases has been the degradation of aquatic ecosystems. Thus, many efforts are now focused on restoring rivers to a more natural state to recover the benefits provided by properly functioning ecosystems (Bernhardt and Palmer, 2007). Revegetating riparian zones, which exist at the interface between land and a stream, is a common restoration action because of the resulting ecosystem benefits including the creation of wildlife habitat and improvement of water quality. However, characterizing frictional resistance of channel boundaries on flow is notoriously difficult to quantify in the presence of woody vegetation (e.g. Barnes, 1967;

Fischenich, 2000; Lightbody and Nepf, 2006), particularly because hydraulic roughness not only is a function of individual plant characteristics and community composition but also varies with water depth and velocity as plants bend and streamline.

Although substantial research has been directed towards exploring vegetated open channel hydraulics and vegetation-fluid interactions, there are at present no comprehensive techniques for predicting vegetation bending in open channels. The goal of this study was to predict the bending behaviour of woody riparian vegetation as a function of hydraulic flow conditions. This was accomplished through a series of field tests to elucidate tree bending properties. The field data served as input parameters for a numerical algorithm designed to predict tree bending for water velocities likely to be encountered during flood events. This study focused on key woody riparian taxa of the southwestern USA; however, the techniques presented here are generic in nature, and analogous data may be collected for additional riparian species in other environments.

\*Correspondence to: M. C. Stone, Department of Civil Engineering, University of New Mexico, Albuquerque, NM 87131, USA.  
E-mail: stone@unm.edu

## LITERATURE REVIEW

Interactions between the flow field and flexible vegetation (henceforth referred to as hydro-vegetation interactions) form a complex, highly dynamic set of processes that are challenging to describe and predict. Here, we provide a brief overview of the numerous studies performed on this topic over the past several decades. We begin by describing the approaches used for defining hydraulic roughness in the presence of vegetation. Next, we summarize research on the influence of vegetation on fluid dynamics and channel hydraulics, followed by the inverse impacts of the hydro-dynamic flow field on channel vegetation. Finally, we summarize previous efforts to characterize and quantify

of vegetation stiffness (Green, 2005), flow depth and velocity (Kouwen and Fathi-Moghadam, 2000), plant density, plant frontal area (e.g. Freeman *et al.*, 2000; Järvelä, 2002; James and Makoa, 2006) and submerged versus emergent plant condition (Wu *et al.* 1999).

Using a force balance analysis, Fischenich (2000) proposed the following resistance relations for emergent and submerged vegetation based on the drag force concept.

$$n = \frac{k_n R^{\frac{1}{6}}}{\left(\frac{U}{u_*}\right) \sqrt{g}} \quad (1)$$

where

$$\frac{U}{u_*} = \begin{cases} \sqrt{\frac{2}{A_{veg} C_D R}} & \text{emergent} \\ \frac{2.5}{H} \left[ \int_0^{h_p} 1.26 h_p^2 \left( \frac{e^{11 C_D A_{veg} z}}{e^{11 C_D A_{veg} h_p}} \right)^{0.5} dz + \int_{h_p}^H \ln \left( \frac{\frac{z}{h_p} - 0.95}{0.13 e^{[-(C_D A_{veg} - 0.4)]^2}} \right) dz \right] & \text{submerged} \end{cases}$$

hydro-vegetation interactions with models and numerical techniques.

#### Hydraulic roughness

Efforts to quantify hydraulic roughness in vegetated channels date back at least to the 1950s and 1960s. The most widely used resistance measure is the Manning's  $n$  coefficient. Manning's  $n$  is typically estimated from narrative descriptions of channel properties (e.g. Chow, 1959), by comparing photographs of rivers with known roughness values (e.g. Barnes, 1967) or through professional judgment. More sophisticated methods split channel resistance into its component parts and use tables to estimate each element separately (e.g. Cowan, 1956). With respect to vegetated channels, the US Soil Conservation Service (now known as the Natural Resources Conservation Service) developed an empirical technique known as the  $n$ -VR approach for calculating roughness of grass-lined channels based on correlations between Manning's  $n$  and the product of velocity ( $V$ ) and hydraulic radius ( $R$ ) (SCS, 1954). This approach has been updated through many subsequent studies including work by Temple (1982) who unified the  $n$ -VR retardance curves.

More recent research has attempted to account for the complex dynamic relationships between the flow field and vegetation-induced roughness. These studies have reported that hydraulic roughness of vegetated channels is a function

In the above equation,  $h_p$  represents the effective vegetation height and is dependent on the degree of bending. Therefore, the ability to predict how a plant bends, or more specifically, how its height changes in the presence of flow, permits more accurate prediction of hydraulic roughness and water surface elevation. Other terms in Equation (1) include the local water depth ( $z$ ), the drag coefficient ( $C_D$ ), the frontal area of the vegetation ( $A_{veg}$ ), the mean velocity ( $U$ ), the shear velocity ( $u_*$ ), the gravitational acceleration ( $g$ ) and a units term ( $k_n$ ). Fischenich and Dudley (2000), Vogel (1994), and Dudley (1997), among others, have provided methods for estimating the terms found in Equation (1), and these are elaborated upon below. This study addresses changes in  $h_p$  as a function of flow velocity.

#### The influence of vegetation on fluid dynamics and channel hydraulics

In addition to investigations into the impacts of vegetation on hydraulic roughness, numerous studies have researched the general impacts of channel vegetation on fluid dynamics and channel hydraulics. Analogous to hydraulic roughness studies, these studies have reported that flow resistance, as investigated through the logarithmic velocity profile, also is a function of the vegetation height, density and stiffness (Kouwen *et al.*, 1969; Kouwen and Li, 1980; Kouwen and Unny, 1973; Kouwen, 1988). Using flume experimental data for artificial flexible roughness elements,

Kouwen and Li (1980) proposed relationships for calculating the roughness height ( $k$ ) of vegetation:

$$k = 0.14h \left[ \frac{(MEI/\tau_0)^{0.25}}{h} \right]^{1.59} \quad (2)$$

where  $h$  is the undeflected roughness height,  $M$  is the density of vegetation per unit area,  $E$  is the modulus of elasticity,  $I$  is the second moment of area and  $\tau_0 = \gamma RS_0$  is the total boundary shear stress (where  $\gamma$  is the fluid specific weight,  $R$  is the hydraulic radius and  $S_0$  is the channel slope). Kouwen and others (Kouwen and Li, 1980; Kouwen, 1988) treated the product of  $M$ ,  $E$  and  $I$  as a single quantifiable parameter ( $MEI$ ) to represent the rigidity of vegetation per unit area and provided  $MEI$  values for common vegetation. However, this empirically derived equation was based entirely on artificial flexible roughness elements under limited hydraulic conditions.

Nepf and Ghisalberti (2008) provide a thorough literature review and conceptual model for the influence of submerged channel vegetation on turbulence structure, mean velocity profiles and dispersion. Wilson *et al.* (2003) investigated the impact of flexible vegetation on open channel flow structure and found that within the plant layer, the velocity profile did not follow the logarithmic law profile, and the mean velocity for an artificial plant canopy without foliage was less than half of that observed for a simple rod array. Velocity measurements showed that the velocity distribution in the vegetation layer was close to a linear profile. Results also indicated that greater momentum absorbing area had a significant effect on mean velocity of the entire channel. Several other studies have reported on the velocity profile within and above both emergent and submerged vegetation (e.g. Järvelä, 2005; Stephan and Gutknecht, 2002).

#### *The influence of fluid dynamics on channel vegetation*

Unlike the studies described above, which focus on the influence of vegetation on the flow field, several flume and wind tunnel studies have been conducted to elucidate the influence of flowing fluids on vegetation. Forces acting on vegetation can be coarsely divided into those applied to bend vegetation (drag and gravitational forces) and those resisting bending (stem and root-soil resistance) (Peltola, 2006). Under steady, uniform flow, the drag-induced moment may be expressed functionally as follows:

$$M_{drag} = f(h, \rho, \mu, g, C_d(y), A_{veg}(y), V(y)) \quad (3)$$

where  $M_{drag}$  is the moment induced by the hydraulic drag force ( $F_{drag} = 1/2\rho C_d A_{veg} V^2$ ),  $y$  is the vertical location

on the plant above the channel bottom,  $\rho$  is the fluid density,  $\mu$  is the dynamic viscosity of the fluid,  $g$  is gravitational acceleration,  $C_d(y)$  is the drag coefficient,  $A_{veg}(y)$  is the frontal area of vegetation exposed to the flowing fluid and  $V(y)$  is the approach velocity of the fluid. It should be emphasized that  $C_d$ ,  $A_{veg}$ , and  $V$  are all functions of vertical distance from the channel bottom,  $y$ .

The drag force equation becomes problematic in dealing with porous, flexible vegetation that can bend and whose frontal area decreases with increasing fluid velocity. With respect to frontal area, wind tunnel and flume experiments have provided estimates of how vegetation streamlines for different types of vegetation under a range of flow conditions (e.g. Freeman *et al.*, 2000; Rudnicki *et al.*, 2004; Vollsinger *et al.*, 2005; Lightbody and Nepf, 2006). Frontal area reductions as high as 54% have been reported for high-velocity environments (Rudnicki *et al.*, 2004). With respect to drag coefficients ( $C_d$ ) for emergent vegetation, it often is assumed that  $C_d$  is constant over the height of the vegetation by presuming that the vertical variation in projected area of the obstruction can be neglected (Lightbody and Nepf, 2006), although more sophisticated routines have been proposed for describing the longitudinal and vertical variations in  $C_d$  (Dunn *et al.*, 1996). An extensive flume study conducted by Freeman *et al.* (2000) reported that plant bending and streamlining resulted in a significant decrease in the drag coefficient with velocity. Wilson *et al.* (2003) investigated drag forces and flow field characteristics through flexible vegetation with and without foliage and found that plant foliage induced higher drag forces but reduced shear-generated turbulence because of an inhibition of momentum exchange by the foliage surface area.

The net gravitational moment ( $M_{gravity}$ , plant weight minus buoyancy) acting on vegetation varies with the force of gravity acting on the tree as it bends. Net gravitational forces have been assumed to be negligible in this study because the specific gravities of riparian trees are near unity, and thus, submerged portions provide a negligible moment because of counteracting buoyancy forces. As such, gravitational forces are neglected in the present analysis but should be further investigated in future research.

Stem resistance refers to properties of a plant associated with stem bending, which are established by examining the plant's material properties. Application of elastic beam theory leads to the following functional form of stem resistive moment for bending.

$$M_{stem} = f(y, \theta, d_{tree}(y), h_{tree}, E_y) \quad (4)$$

where  $M_{stem}$  is the moment of stem resistance,  $\theta$  is the deflected angle of departure from vertical,  $d_{tree}(y)$  is the stem diameter,  $h_{tree}$  is the total tree height and  $E$  is the modulus of elasticity of the tree.

Root-soil resistance is dependent upon the physical characteristics of the site surrounding the plant and the root characteristics. Site characteristics influencing resistance to bending include local topography and slope, and soil properties such as texture, bulk density and soil moisture.

#### Modelling hydro-vegetation interactions

Conceptual and numerical models can provide insights into the complex hydro-vegetation interactions and improve predictive capability of engineering models. A small number of studies have been conducted with respect to the mechanical response of vegetation, bending and/or breakage, under different flow conditions. Groeneveld and French (1995) conducted field investigations to examine the critical velocity required to rupture emerging tule stems. They applied a drag force approach to analyse the mechanical properties of a single stem plant in flowing water and developed the critical condition for stem rupture. Based on this method, Duan *et al.* (2002) conducted a more detailed analysis for the flow-plant mechanics for a plant with a vertically varying diameter. This study was restricted to the nonbending condition. Chen and Stone (2010) provided an alternative numerical approach for describing vegetation bending under static and dynamic conditions for tapered vegetation exposed to a user defined velocity profile.

## METHODS

The goal of this study was to predict the bending behaviour of woody riparian vegetation as a function of hydraulic flow conditions, which was accomplished through the following objectives: (i) describe *in situ* biomechanical properties of common woody riparian vegetation species of the southwestern USA; (ii) develop a technique for predicting bending characteristics of submerged vegetation; and (iii) estimate the extent of bending for common woody riparian vegetation species under a range of hydraulic conditions. These research objectives were accomplished through a series of field studies to elucidate tree-bending properties that were then used as input parameters for a numerical algorithm designed to predict tree bending in a moving fluid.

#### Site and specimen selection

Field sites were chosen throughout the southwestern USA with a focus on sites with similar riparian species composition but with a sufficiently large array of other environmental conditions. Based on vegetation surveys conducted throughout the region and availability of hydraulic drag characteristics, the following taxonomic groups were deemed frequent and relevant for targeting in the experimental design: willows (*Salix spp.*), cottonwoods (*Populus spp.*) and salt cedars

(*Tamarix spp.*). Willows and salt cedars have a bush-like morphology with slender stems that form thickets. Cottonwood trees have a clearly defined main trunk with large wide-spreading limbs that can produce a broad crown. The field sites included the following: the San Luis Rey River in Oceanside, California; the Las Vegas Wash near Las Vegas, Nevada; and the Rio Grande in Albuquerque, New Mexico. Detailed descriptions of these sites can be found in Goreham (2009). The individual specimens were selected to provide a range of characteristics including tree size and age. Logistical constraints including accessibility and landowner permission to access the site also played a considerable role in specimen selection.

#### Field tests

To predict vegetation bending as a function of hydraulic flow conditions, the tree's modulus of elasticity ( $E$ ), second moment of area ( $I$ ) and frontal area ( $A_{veg}$ ) must be known.  $A_{veg}$  was measured directly using digital image processing.  $I$  was calculated from caliper measurements of tree diameter assuming a cylindrical cross section ( $I = \pi d^4 / 64$ ). Tree pulling tests were conducted to elucidate  $E$  values for study taxa.

Vegetation bending was induced by exerting force via an anchored tree pulling apparatus (Figure 1). Testing protocols were adapted to riparian environments from methods used in tree stability testing in silvicultural forests (Peltola, 2006; Nicoll *et al.*, 2006). The experimental design used a three-quarter-ton truck and mounted ATV winch for applying the force. A strain gauge was used to measure the applied force, and digital inclinometers collected pulling and bending angles. For consistency, force was applied at approximately one-third of the total tree height for all specimens. Prior to each test, a suite of background parameters was collected, including the following: individual vegetation characterization, site properties and test conditions.

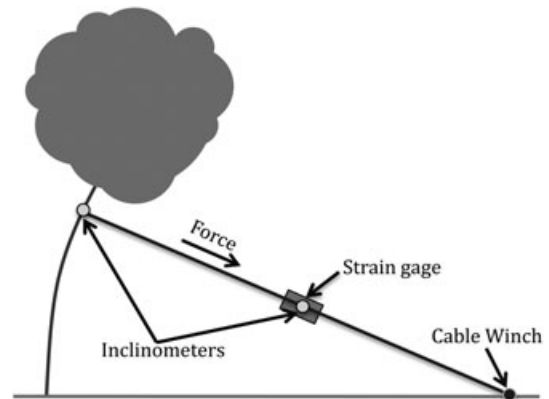


Figure 1. Schematic representation of the vegetation pulling apparatus.

Figure 2 provides a typical dataset for a cottonwood pull test describing the bending response of the tree as an increasing level of force was applied. In this particular case, the tree deflection angle increased to approximately 26 degrees at a point when a force of approximately 4000 N was applied.

Next, the bulk modulus of elasticity was determined for each specimen by employing elastic beam theory while treating the tree as a cantilever member [Equation (5)]. This invokes the following assumptions: (i) the trunk is assumed to be a cylindrical cantilever beam; (ii) the material properties are homogeneous and isotropic; and (iii) deformation is caused by bending only without shear.

$$\frac{\frac{d^2x}{dy^2}}{\left[1 + \left(\frac{dx}{dy}\right)^2\right]^{\frac{3}{2}}} = \frac{M}{EI} \tag{5}$$

where  $x$  is the distance in the streamwise or deflected direction,  $y$  is the vertical distance above the channel bottom for a point on the tree and  $M$  is the internal bending moment. This equation represents a nonlinear second-order differential equation. Solution of Equation (5) gives the exact shape of the elastic curve,  $x = f(y)$ . When restricted to small deflections (i.e. early in the pulling tests),  $dx/dy$  is approximately zero. Consequently, its square is negligible compared with unity, and Equation (5) reduces to the following linear differential equation:

$$\frac{d^2x}{dy^2} = \frac{M}{EI} \tag{6}$$

For a concentrated load at the free end of the beam, integration of Equation (6) and rearranging to solve for  $E$  gives the following:

$$E = \frac{FL^2}{2I\theta_{max}} \text{ at } x = L \tag{7}$$

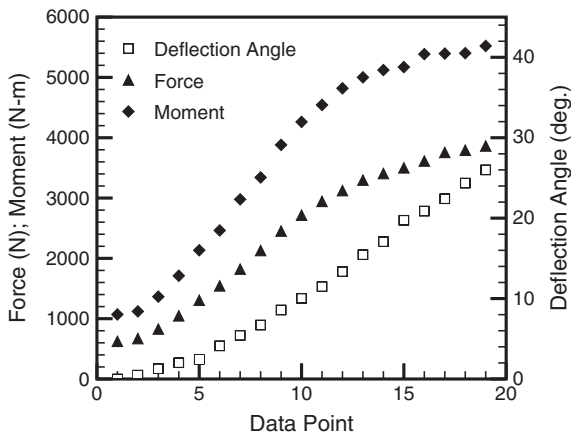


Figure 2. Example of pulling test data from a SLR cottonwood.

where  $\theta_{max}$  is the maximum slope of the beam,  $F$  is the force applied normal to the beam and  $L$  is the beam length. All terms on the right-hand side of Equation (7) were measured directly during field tests, and thus,  $E$  was calculated for each specimen.

*Vegetation-bending predictions*

Unlike the application of elastic beam theory for small deflections employed for the determination of  $E$ , vegetation exposed to high flows will undergo large deflections. The governing elastic beam theory equation for large deflections becomes considerably more complicated as the beam now experiences both horizontal and vertical displacement. More specifically, the denominator of Equation (5) cannot be reduced to unity as was the case with small deflections. Thus, estimating the degree of vegetation bending requires an approach that accounts for large deflection. Ang Jr. *et al.* (1993) presented a numerical method applying a search procedure to solve the large deflection cantilever problem resulting from the application of a concentrated load at the beam’s end. Chen (2010) and Chen and Stone (2010) proposed a new approach based on the formulation by Ang Jr. *et al.* (1993) capable of predicting large deflections for tapered, cylindrical cantilevers subjected to user specified loads. Based on this approach, Equation (5) can be integrated and converted to the following:

$$\frac{ds}{dy} = \frac{1}{\sqrt{1 - G^2(y)}} \tag{8}$$

where  $s$  is the distance measured along the beam from the fixed end, and function  $G(y)$  is defined by  $G(y) = \int_0^y \frac{M(y)}{EI} dy$

Equation (8) is a general equation that can be applied to an arbitrary load and to complex beam properties (e.g. non-uniform cross-sectional area and nonuniform rigidity). For uniform beams with specific load distributions,  $G(y)$  may be explicitly integrated based on the expression of  $M(y)$ . For instance, for a total load  $P$  uniformly distributed along the deflected beam length  $h$ , we have  $M(y) = \frac{P}{2h}(h - y)^2$  and  $G(y) = \frac{P}{2EI} \left( \frac{y^3}{3h} - y^2 + hy^2 \right)$ . For a general case,  $G(y)$  can be numerically discretized on elements. Equation (8) can then be solved with numerical integration to find the bending curve and all quantities of interest. In general, a search or an iterative procedure is adopted to determine the deflected beam length  $l$  and the specific shape of the bending curve. For the uniform load case, a scan of  $h$  values can be performed to satisfy the total beam length at  $y=h$ , which equals  $L$  (i.e.  $s(h) = \int_0^{s(h)} ds = L$ ). This holds regardless of whether  $P$  is a constant or a function of  $s$ . For a general case, an iterative procedure is more effective (Chen, 2010).

The Chen and Stone algorithm requires an estimate of the drag force experienced by the tree ( $F_d$ ), the tree's modulus of elasticity ( $E$ ), the nonstreamlined tree height ( $L$ ), the diameter of the trunk at the base ( $D_0$ ) and the degree to which the trunk is tapered ( $T$ ), as input parameters. The algorithm produces the reduced height of the tree because of bending ( $h$ ), the entire tree profile and the maximum angle of deflection ( $\theta_{max}$ ).

Prediction of vegetation bending as a function of hydraulic flow conditions requires an estimate of the drag force ( $F_d$ ) exerted on the object for a given water velocity. Calculation of  $F_d$  requires an estimation of vegetation area normal to the flow ( $A_{veg}$ ). Studies investigating changes in  $A_{veg}$  as a function of fluid velocity are scarce. Vollsinger *et al.* (2005) conducted wind tunnel measurements of tree crown streamlining for several hardwood species common to northwestern North America. Their study described the relationship of frontal area ratio ( $A_r$ ) (streamlined frontal area/non-streamlined frontal area) of the crowns of five different tree species using digitized video images. In a flume study designed to elucidate hydraulic roughness values for shrubs and other flexible vegetation, Freeman *et al.* (2000) observed maximum streamlining of vegetation at a water velocity of about  $1.2 \text{ m}\cdot\text{s}^{-1}$ , where the term 'maximum streamlining' refers to no significant decrease in  $A_r$  with increasing velocity. In this study, the relationships proposed by both Vollsinger *et al.* (2005) and Freeman *et al.* (2000) were used and compared to estimate the influence of tree crown streamlining on vegetation bending.

To determine the nonstreamlined tree frontal area ( $A_{veg}$ ), scaled digital photographs of each specimen were taken prior to bending tests.  $A_{veg}$  and  $L$  were then determined using Adobe Photoshop<sup>®</sup> and ImageJ software packages. Vollsinger *et al.* (2005) observed that the dynamic  $C_d$  was relatively constant at a value of 0.60 above an equivalent water velocity of  $0.55 \text{ m}\cdot\text{s}^{-1}$  for all species. Accordingly, we used this value for the drag coefficient for computing drag forces as this study is concerned primarily with high flows (i.e.  $V_{water} \geq 0.5 \text{ m}\cdot\text{s}^{-1}$ ). However, a sensitivity analysis was performed to elucidate the effect of  $C_d$  and  $A_{veg}$  variability on vegetation bending. Having established a strategy for the calculation of  $A_{veg}$  and  $C_d$ , the drag force experienced by a tree could then be determined using the drag force equation. The drag force estimates were used to estimate loading and internal bending moments along the height of the tree. The algorithm used this information to describe the degree of deflection for the given specimen and flow field characteristics.

With respect to the vegetation-bending simulations, the following general assumptions were made: (i) only the submerged condition was considered (i.e. flow depth > tree height); (ii) only a single tree was considered; and (iii) the hydraulic drag force was assumed to be distributed

uniformly over the length of the tree. These assumptions will be addressed in future research.

## RESULTS

Through the field observations, vegetation properties were collected for 26 total specimens from three field sites including 6 cottonwoods, 12 willows and 8 salt cedars. Data collected from the tree pulling experiments were used to calculate values for  $A_{veg}$ ,  $I$  and  $E$  for each tree. Drag forces and resultant bending were estimated for each tree for five water velocities ( $0.5$ ,  $1.0$ ,  $1.5$ ,  $2.0$  and  $2.5 \text{ m}\cdot\text{s}^{-1}$ ).

### Modulus of elasticity

Although a range of data was produced to estimate vegetation bending, the modulus of elasticity,  $E$ , is the primary variable that is generalizable to other studies and locations and thus is presented in Figure 3 and Table 1 as grouped by genus. The white boxes represent the mean values, the black boxes represent the SDs, and the whiskers represent the minimum and maximum values. A large degree of variation was observed both between and within vegetation types. The degree of variation within specimens was much larger than that typically observed when conducting equivalent experiments on manufactured materials in the laboratory, but this was not unexpected when considering the high degree of variability in the specimens themselves along with the environments in which they were observed. The variation between vegetation types was investigated statistically using a one-way ANOVA to examine whether  $E$  changed as a function of vegetation type. The results revealed a significant difference in the mean  $E$  between species,  $F(2,23)=4.865$ ,  $p < 0.05$ . Post hoc analyses revealed that the mean elasticity of salt cedar was significantly lower than that of cottonwood,  $t(2,12)=2.184$ ,  $p < 0.05$ , and that of

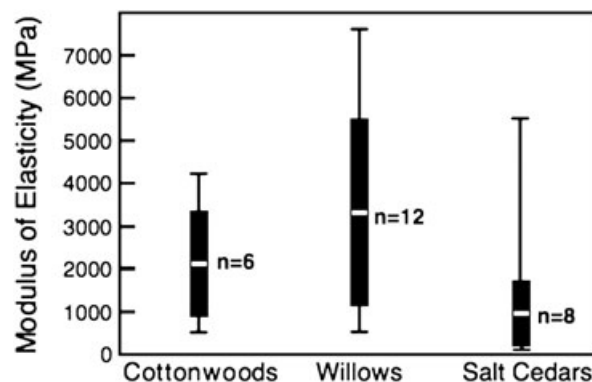


Figure 3. Modulus of elasticity for each vegetation type. The white boxes represent mean values, the black boxes represent the SD, and the whiskers indicate maximum and minimum values.

Table I. Summary of vegetation properties from field observations

Species	Metric	H (m)	A (m <sup>2</sup> )	I (m <sup>4</sup> )	E (MPa)	EI (kN m <sup>2</sup> )
Cottonwood	Average	5.7	5.0	2.22725E-05	2129	47.4
	SD	2.1	4.1	2.43872E-05	1230	
Willow	Average	5.6	3.8	9.62155E-06	3323	32.0
	SD	2.7	4.4	1.6787E-05	2175	
Salt cedar	Average	3.5	4.7	5.9E-05	966	56.7
	SD	1.0	6.1	1.6E-04	766	

willow,  $t(2,15)=3.446$ ,  $p < 0.005$ . There was not a statistically significance difference in elasticity between cottonwood and willow,  $t(2,16)=1.237$ ,  $p=0.234$ .  $E$  did not correlate with any of the other plant characteristics that were measured in this study (e.g. trunk diameter, height and crown area). This does not rule out potential correlations with other unmeasured plant characteristics such as specimen age or stem water content, which should be investigated through future research.

#### Vegetation-bending algorithm

The vegetation-bending algorithm developed by Ang Jr. (1993) and adapted by Chen (2010) and Chen and Stone (2010) was used to predict plant deflection under a range of flows. First, however, the model was tested using the field observations of tree deflection for a measured load. Recall, the  $E$  values were determined based on simplified elastic beam theory for minor deflection using Equation (6), which is a linear differential equation. On the other hand, the deflection results are based on the solution of the integrated form [Equation (8)] of the fundamental elastic beam theory equation [Equation (5)], which is a nonlinear second-order differential equation. Thus, a comparison between the observed and simulated deflection results provide an independent test of the algorithm's capabilities. Because the field

tests were applied as a point load, the same configuration was applied for these tests, whereas a distributed load was used for the hydrodynamic tests described below.

Figure 4 contains model performance data in the form of the deflection angle predicted by the model plotted against the observed deflection angle measured with a vertical inclinometer. A 1:1 line is included to indicate the condition of perfect agreement. The model performed well with respect to its ability to reproduce the observed deflection angle with a root mean square error of 2.3°. The modelled data more closely matched the observed data at lower deflection angles, whereas larger discrepancies were observed at higher angles. No clear bias for overpredicting or underpredicting was observed.

#### Vegetation deflection

The vegetation bending characteristics for all 26 specimens were estimated for flow velocities ranging from 0.5 to 2.5 m·s<sup>-1</sup> using the vegetation-bending algorithm. A drag force was estimated for each specimen and velocity combination using the techniques described above and the data collected in the field. The detailed results for all 26 specimens can be found in Goreham (2009). Figure 5 contains the results of typical cottonwood, willow and salt cedar specimens. These specific specimens were selected simply because they had similar initial heights and areas. As expected, the degree of deflection increased in all cases as a function of the approach velocity. The rate of change in deflection as a function of velocity decreased at higher velocities. Thus, the profiles for 2.0 m·s<sup>-1</sup> were omitted from the figure because they were nearly indistinguishable from the 2.5 m·s<sup>-1</sup> profiles. For the specific specimens shown in Figure 5, the degree of deflection was similar between the three vegetation types, with the salt cedar deflected the least and the willow the most. This result appears to contradict what one would expect from the  $E$  results provided in Figure 3. This apparent discrepancy can be used to better understanding the physical interpretation of the terms within the deflection algorithm. Equation (8) indicates that the overall plant rigidity (resistance to deflection) is represented by the product of  $E$  and  $I$ . The results displayed in

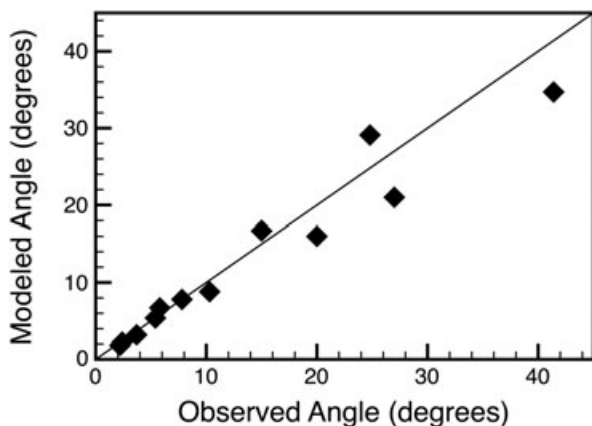


Figure 4. Modelled deflection angle versus observed deflection angle.

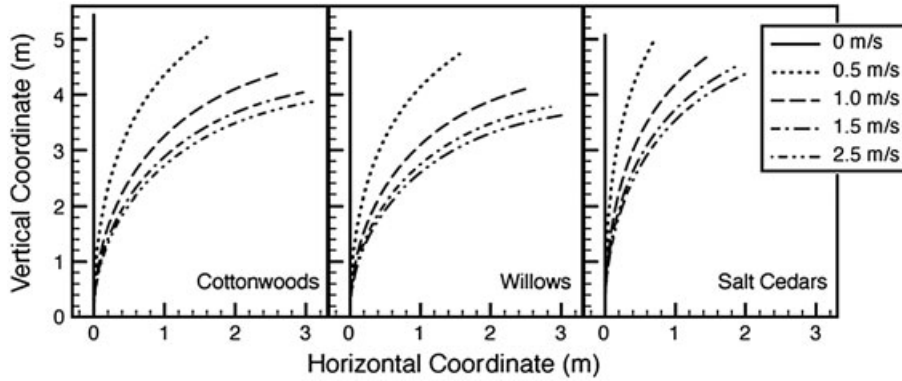


Figure 5. Example of modelled bending profile as a function of flow velocity and vegetation species.

Figure 5 are consistent with the mean products of  $EI$  (see Table 1) where salt cedar specimens were the most rigid (high  $EI$ ), followed by cottonwoods and then willows.

*Vegetation height ratios*

The degree to which the flow influences a plant specimen can be investigated through the deflected specimen's height ratio,  $H_r$ , defined as the deflected plant height divided by the original plant height ( $h/L$ ). Figure 6 depicts predicted height ratios broken down by vegetation type. The boxes represent the mean  $H_r$  and the whiskers represent minimum and maximum values. As was the case for  $E$ , substantial variation was observed between specimens. Consistent with the vegetation profiles shown in Figure 5, the degree of bending increased with velocity, but the rate of change slowed substantially at higher velocities. The results also were consistent with the  $E$  observations in that  $H_r$  values were smallest for salt cedars (high degree of bending) and largest for willows (low degree of bending). The mean  $H_r$  was above 0.6 for all three vegetation types at a velocity of  $2.5 \text{ m}\cdot\text{s}^{-1}$ , but a minimum  $H_r$  value of 0.42 was observed for a single salt cedar specimen.

To examine the effects of velocity on  $H_r$  between species, a  $5$  (velocity)  $\times$   $3$  (vegetation type) factorial ANOVA was conducted. The main effect of velocity on  $H_r$  was significant,  $F(4,85) = 15.097$ ,  $p < 0.001$ .  $R^2 = 0.439$ . Although bending behaviour between species was observed to be different, the ANOVA revealed that there was no statistically significant difference in  $H_r$  between vegetation type,  $F(2,85) = 1.747$ ,  $p = 0.181$ .

*Sensitivity analysis*

As described in the methods section, application of the vegetation-bending algorithm to actual tree specimens required several important assumptions including estimates of the degree of vegetation streamlining ( $A_r$ ) and the vegetation drag coefficient ( $C_d$ ). Hence, a sensitivity analysis was conducted to determine whether these assumptions had a significant effect on the bending results. First, because  $A_r$  was estimated based on the experimental results provided by Vollsinger *et al.* (2005) and because their data displayed substantial scatter, we investigated the sensitivity of our study results to the selection of  $A_r$ . This was accomplished by comparing the deflection results based on the mean,

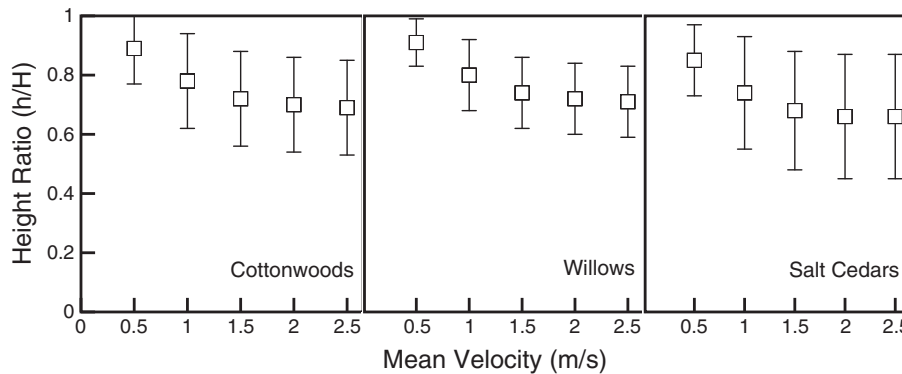


Figure 6. Summary of height ratios as a function of flow velocity and vegetation species. The boxes represent mean values, and the whiskers represent minimum and maximum values.

maximum, and minimum  $A_r$  values reported by Vollsinger *et al.* (2005). The results of a one-way ANOVA indicated that there was no statistically significant difference between the resulting  $H_r$  because of the method of selection for  $A_r$ ,  $F(2,42) = 1.748$ ,  $p = 0.187$ .

Selection of  $C_d$  introduces another source of potential uncertainty into the study results. A one-way ANOVA was conducted to investigate the sensitivity of  $H_r$  to  $C_d$  by varying  $C_d$  from its default value of 0.6 to minimum and maximum values of 0.5 and 0.7, respectively. These values are consistent with the range of dynamic  $C_d$  values reported by Vollsinger *et al.* (2005). The results showed that there was no statistically significant difference in  $H_r$  values between different  $C_d$  values,  $F(2,42) = 0.729$ ,  $p = 0.489$ . Therefore, reasonable but differing choices for  $C_d$  and  $A_r$  are unlikely to elicit substantially different tree bending predictions.

## DISCUSSION

The results from the field observations and numerical bending experiments provide an improved understanding of the material properties of *in situ* riparian trees and the potential extent of tree bending during floods. The results serve the goal of this research, which was to predict the bending behaviour of woody riparian vegetation as a function of hydraulic flow conditions.

With respect to the first study objective, describing the biomechanical properties of common woody riparian vegetation species, this research revealed a high degree of variability in  $E$  between and within vegetation types. Although all observations were within an order of magnitude, the maximum values were five to six times higher than the minimum values with the greatest variability observed for willows. To some extent, a wide degree of variation in such properties is expected for biological specimens. However, the logistical complexity and resources required to collect *in situ* bending data severely limited the size of our dataset and thus prevented a more thorough investigation of the variables that potentially play a role in this variability. In spite of the substantial variability among vegetation types, the  $E$  values for salt cedars were still found to be significantly less than those for willows and cottonwoods. Willows had a higher mean  $E$  than cottonwood specimens, but the difference was not found to be significant.

The second objective of this research was to develop a technique for predicting the bending characteristics of riparian vegetation. To accomplish this objective, the vegetation-bending algorithm described by Chen (2010) and Chen and Stone (2010) and based on Ang Jr.'s (1993) method for describing a highly deflected cantilever system was applied. The algorithm was modified to account for tapered vegetation

and distributed loads. The vegetation-bending algorithm performed well in a comparison between predicted and measured deflection angles. Although the current algorithm includes several key assumptions, this tool provides an important initial step in our ability to predict deformation of vegetation because of flowing fluids.

The vegetation-bending algorithm was applied to satisfy the third study objective, which was to estimate the extent of bending for common woody riparian vegetation species under a range of hydraulic conditions. A total of 130 numerical bending experiments (26 specimens  $\times$  5 flow velocities) were conducted to study the extent of bending within and between vegetation types. Although complete plant profiles were produced for each test, the results were summarized with respect to the height ratio ( $H_r$ ) under each flow condition. The simulations revealed a high degree of variability within vegetation types and moderate variability between vegetation types. The variability between vegetation types was not found to be statistically significant. The marginal nature of the statistics could be caused by the high degree of variability and relatively low sample number within each vegetation type.

### *Implications for river management*

Estimating hydraulic roughness in the presence of channel or floodplain vegetation has always been a challenge in river engineering. In many instances, this problem has been avoided by eliminating vegetation in vulnerable areas. Today, however, the multiple benefits provided by vegetation are more fully recognized, and the protection, enhancement and restoration of riparian vegetation often are encouraged or even mandated. One of the challenges in accounting for woody riparian vegetation in hydraulic assessments is the lack of knowledge of how vegetation will deform under different flow conditions. The results of this study provide a general approach for predicting vegetation-bending behaviour along with estimates of the extent of bending for several common woody vegetation types.

Extension of the study results to investigate impacts on hydraulic roughness requires the consideration of plant morphology, composition and density. The shrub-like or bush-like plant morphology of salt cedars will influence the flow field differently than the tree-like or canopy morphology of cottonwood trees. Willow morphology falls somewhere between the other two. Depending on the depth of flooding, only the submerged portion of the plant will produce drag, and hence, a physical investigation of the influence of roughness must include a function of flow depth for plant characteristics. The vegetation-bending algorithm presented here was designed with this logic in mind, but this step is left for future research.

### Future research

The complexity of the question at hand, and the logistical challenges in collecting *in situ* biomechanical data and estimating vegetation bending, required several simplifying assumptions throughout the project. Hence, several opportunities remain for advancing this line of research. With respect to field observations, we have presented an innovative approach for describing *in situ* vegetation properties, most notably the modulus of elasticity. Although efficiency was gained throughout field observations, the process is still logistically challenging and arduous. Hence, a major limitation to our work was the limited number of specimens for each vegetation type, which prevented a thorough analysis of the correlations and covariances within study variables. For example, within a vegetation type,  $E$  is likely influenced by plant age. Thus, an important focus of future research should be to gather a much larger dataset to facilitate the investigation of such relationships.

The vegetation-bending algorithm provides an innovative, physically based method for studying plant deflection. However, several major simplifying assumptions were made in the current algorithm including treatment of the vegetation as a cantilever system and distribution of the drag force as a uniform load. Furthermore, only the case of submerged vegetation was investigated, and the simulations were carried out for single specimens. Clearly, these assumptions should be revisited, and additional capabilities should be added as needed. As discussed above, the capability of simulating emergent vegetation with vegetation characteristics as a function of height would facilitate investigations of hydraulic roughness.

Application of the field data and vegetation-bending algorithm required several assumptions to predict bending behaviour. For example, the drag coefficient and extent of vegetation streamlining were based on data from the literature and assumed to be the same for all vegetation types. Although a sensitivity analysis revealed that these assumptions did not significantly influence the study results, additional studies to describe these variables for the vegetation types and conditions of specific interests would reduce uncertainty in the final models.

Finally, this research would benefit greatly from field verification of vegetation bending under high flows. This type of data is obviously difficult and usually dangerous to obtain because of the very nature of flood events. However, such data could potentially be obtained during controlled floods or through indirect observations. Post-flood observations also can provide some insights into the influence of flood flows on vegetation.

### REFERENCES

- Ang Jr MH, Wang W, Low TS. 1993. On the estimation of the large deflection of a cantilever beam. *Proceedings of the IEEE IES Annual Conference IECON'93 Hawaii USA*: 1604–1609.
- Barnes HH. 1967. Roughness Characteristics of Natural Channels: US Geological Survey Water Supply Paper 1849. *US Geological Survey*.
- Bernhardt ES, Palmer MA. 2007. Restoring streams in an urban context. *Freshwater Biology* **52**: 738–751.
- Chen, L. 2010. An Integral Approach for Large Deflection Cantilever Beams. *International Journal of Non-Linear Mechanics* **45**: 301–305.
- Chen L, Stone MC. 2010. Theoretical analyses for the interaction between vegetation bending and flow. *World Water & Environmental Resources Congress ASCE*. American Society of Civil Engineers: Providence RI.
- Chow VT. 1959. *Open-Channel Hydraulics*. McGraw-Hill: New York, NY.
- Cowan WL. 1956. Estimating Hydraulic Roughness Coefficients. *Agricultural Engineering* **37**: 473–475.
- Duan G, French RH, Miller J. 2002. The lodging velocity for emergent aquatic plants in open channels. *Journal of the American Water Resources Association* **38**: 255–263.
- Dudley SJ. 1997. *Vegetation measurements for predicting flow resistance*. Ph.D. Dissertation. Colorado State University Fort Collins Colorado: Fort Collins, CO.
- Dunn C, López F, García M. 1996. Mean flow and turbulence in a laboratory channel with simulated vegetation. *Hydraulic Engineering Series No. 51 UILU-ENG-96-2009*. Department of Civil Engineering University of Illinois Urbana-Champaign: Urbana-Champaign, IL.
- Fischenich JC. 2000. Resistance due to vegetation. *ERDC TN-EMRRP-SR-07*. Engineer Research and Development Center Vicksburg Mississippi.
- Fischenich C, Dudley S. 2000. *Determining drag coefficients and area for vegetation*. Army Corps of Engineers: U.S..
- Freeman GE, Rahmeyer WH, Copeland RR. 2000. Determination of resistance due to shrubs and woody Vegetation. *ERDC/CHL TR-00-25*. U.S. Army Engineer Research and Development Center Vicksburg Mississippi.
- Goreham JO. 2009. *Bending of woody riparian vegetation as a function of hydraulic flow conditions*. University of Nevada Las Vegas Masters Thesis: Las Vegas Nevada USA.
- Green J. 2005. Modelling flow resistance in vegetated streams: review and development of new theory. *Hydrological Process* **19**: 1245–1259.
- Groeneveld DP, French RH. 1995. Hydrodynamic control of an emergent aquatic plant (*Scirpus Acutus*) in Open Channels. *Water Resources Bulletin* **31**: 505–514.
- James CS, Makoa MJ. 2006. Conveyance estimation for channels with emergent vegetation boundaries. *Institution of Civil Engineers. Proceedings. Water Management* **159**: 235–243.
- Järvelä J. 2002. Flow resistance of flexible and stiff vegetation: A flume study with natural plants. *Journal of Hydrology* **269**: 44–54.
- Järvelä J. 2005. Effect of submerged flexible vegetation on flow structure and resistance. *Journal of Hydrology* **307**: 233–241.
- Kouwen N. 1988. Field Estimation of the Biomechanical Properties of Grass. *Journal of Hydraulic Research* **26**: 559.
- Kouwen N, Li RM. 1980. Biomechanics of vegetative channel linings. *Journal of the Hydraulics Division* **106**: 1085–1103.
- Kouwen N, Fathi-Moghadam M. 2000. Friction factors for coniferous trees along rivers. *Journal of Hydraulic Engineering ASCE* **126**: 732–740.
- Kouwen N, Unny TE, Hill HM. 1969. Flow resistance in vegetated channels. *Journal of the Irrigation and Drainage Division. ASCE* **95**: 329–343.
- Kouwen N, Unny TE. 1973. Flexible roughness in open channels. *Journal of Hydraulic Engineering* **99**: 713–728.
- Lightbody AF, Nepf HM. 2006. Prediction of velocity profiles and longitudinal dispersion in emergent salt marsh vegetation. *Limnology and Oceanography* **5**: 218–228.
- Nepf HM, Ghisalberti M. 2008. Flow and transport in channels with submerged vegetation. *Acta Geophysica* **56**: 753–777.
- Nicoll BC, Gardiner BA, Rayner B, Peace AJ. 2006. Anchorage of coniferous trees in relation to species soil type and rooting depth. *Canadian Journal of Forest Research. NRC Canada*. **36**: 1871–1883.
- Peltola HM. 2006. Mechanical stability of trees under static loads. *American Journal of Botany* **93**: 1501–1511.

## BENDING OF SUBMERGED WOODY RIPARIAN VEGETATION

- Rudnicki M, Mitchell SJ, Novak MD. 2004. Wind tunnel measurements of crown streamlining and drag relationships for three conifer species. *Canadian Journal of Forestry Research* **34**: 666–676.
- Soil Conservation Service. 1954. Handbook of channel design for soil and water conservation. *SCS-TP-61 Stillwater Outdoor Hydraulic Laboratory Stillwater Oklahoma*: Stillwater, OK.
- Stephan U, Gutknecht D. 2002. Hydraulic resistance of submerged flexible vegetation. *Journal of Hydrology* **269**: 27–43.
- Temple DM. 1982. Flow retardance of submerged grass channel linings. *Transactions of the American Society of Agricultural Engineers*: St. Joseph, MI; **25**(5): 1300–1303.
- Vogel S 1994. *Life in moving fluids: The physical biology of flow*. Princeton University Press: Princeton NJ.
- Vollsinger S, Mitchell SJ, Byrne KE, Novak MD, Rudnicki M. 2005. Wind tunnel measurements of crown streamlining and drag relationships for several hardwood species. *Canadian Journal of Forest Research* **35**: 1238–1249.
- Wilson CAME, Stoesser T, Bates PD, Pinzen AB. 2003. Open channel flow through different forms of submerged flexible vegetation. *Journal of Hydraulic Engineering ASCE* **129**: 847–853.
- Wu F, Shen HW and Chou Y. 1999. Variation of roughness coefficients for unsubmerged and submerged vegetation. *Journal of Hydraulic Engineering* **125**: 934.